

## Effect of Structural Transformation on the Mechanical and Electrical Properties of Quenched (Pb - 1.5 wt % Sb) Alloy

E. M. Sakr<sup>1</sup>, M. R. Nagy<sup>2</sup> and A. S. Mahmoud<sup>2</sup>

1) University College of Girls, Ain Shams University, Cairo, Egypt

2) Faculty of Education, Ain Shams University, Cairo, Egypt

Creep tests of the quenched (Pb-1.5 wt% Sb) alloy have been carried out under three different constant stresses of 12 MPa, 13 MPa and 15 MPa. Transient and steady state creep of this alloy showed a transition point at 443K. The transient creep parameters ( $\beta$  and  $n$ ) were found to change with the applied stress and ageing temperature. The activation energy of the transient creep ( $Q_{tr}$ ) was found to be 52kJ/mole, and 92kJ/mole, above and below 443 K, respectively. Grain boundary sliding was suggested to be the rate controlling mechanism. Steady state creep of the tested alloy has been investigated around the transformation temperature region. The strain rate sensitivity parameter ( $m$ ) was found to be in the range (0.11 to 0.33), characterizing a cross - slipping and climb dislocation mechanisms. The microstructure analysis showed that the residual internal strain was relatively recovered and segregated in the phase transformation temperature region. Moreover, the temperature dependence of the relative resistivity ( $\rho_t / \rho_o$ ) change was studied. The energy activating the precipitation process ranged from (0.11 to 0.12eV) suggesting the migration of vacancy and antimony solute atom.

### 1. Introduction:

Lead (Pb) is widely used because of its easy formability, low cost, high specific gravity at room temperature. Lead is frequently alloyed with antimony. There is a slight solubility of antimony in Lead, 3.45 wt% Sb, at the eutectic temperature. If the Pb-Sb alloy is quenched the solid solution will be age - hardened, and shows a rise in tensile strength, hardness and endurance limit. Although antimony has deleterious electrochemical, side effects [1, 2], the binary (Pb-Sb) alloy is commonly used in industry, such as the grid metal for Lead-Acidic batteries. This is due to its strengthening role [3], through solid solution and via the dispersion effect of a finely divided eutectic mixture[4], where the load carrying members of the grid must resist creep-type deformation during service.

Lead - based "Babbitt" consisting of hard intermetallics dispersed in a Pb-based solid solution, are also important bearing material. These materials are good for embedding hard contaminant particles and resistance to galling. The addition of antimony is not only used to harden the alloys but also to make them more resistive to compressive impact and wear, and also lowers the casting temperature and minimize contraction during freezing [5, 6]. Quenching alloy samples gives rise to changes in electrical resistivity [7], due to the dispersed solute atoms and the point defects induced by the quenching process.

The change in the steady state rate of Pb-Sb eutectic alloy is studied by [8] under constant stresses ranging from 3.45 to 5.2 MPa and at different temperatures. The strain rate resistivity parameter ( $m$ ) varied between 0.33 and 0.46 in the testing temperature range. The activation energy of the steady state creep amounted to 96 kJ/mole in the temperature range from 473K to 503K, characterizing the self- diffusion mechanism of Pb-Sb.

The quenching techniques and temperature dependence of structural and stress-strain characteristics of deformed Pb-2 wt% Sb alloy during transformation has been studied by Al-Ganainy *et al.* [9]. Tensile strain-strain tests were carried out in the temperature range from 443 to 500 K, there are two different deformation stages around the transformation temperature 437 K.

Creep tests were carried on Pb-1.5 wt% Sb (slow cooled) [10] made under different constant stresses ranging from 12 MPa to 15 MPa near the transformation temperature. Transient and steady state creep of this alloy showed a transition point at 443K. The activation energy of both the transient and steady state creep was found to be 42 kJ/mole and 52 kJ/mole respectively above 443K. The strain rate sensitivity parameter ( $m$ ) has the values ranging from 0.17 to 0.35.

The aim of the present work is to investigate the effect of phase transformation on the mechanical properties of the tested alloy. Variations in the microstructure, due to precipitation and dissolution in the aged samples, are also aimed to be investigated by using x-ray diffraction and electron microscope techniques. The variation of the electrical resistivity at different ageing temperatures was also studied.

## 2. Experimental Techniques:

The tested alloy was prepared from the elements (Pb, 99.9% - Sb, 99.9%) by using an ordinary vertical furnace. It was homogenized at 443K for 72 hours (eutectic temperature), then cold swaged into wires at two diameters ( $5 \times 10^{-4}$  m

and  $1 \times 10^{-3}$  m) and cut to pieces of length ( $5 \times 10^{-2}$  m). The wire samples were annealed at 503K for 2 hours and then rapidly quenched in liquid nitrogen at a cooling rate of  $10^{-3}$  K/sec<sup>-1</sup>. Creep deformations of the tested wires were studied using the apparatus previously described by Sakr [11].

X-ray diffraction patterns of the crept alloy samples were obtained by using a Philips [12] diffractometer. The transmission and scanning electron microscope JEOL/JEM - 100s were utilized for structural investigations. The electrical resistivity changes with temperatures of the test wires were measured using 2-prob-Kelvin double bridge [13].

### 3. Experimental Results and Discussion:

Figure (1) shows the creep curves of (Pb-1.5wt%Sb) under three different applied stresses (12, 13 and 15 MPa) at various ageing temperatures from (413K to 473K) in steps of 10K, and then rapidly quenched in Nitrogen. It is clear from this figure that the slopes of the linear parts of the curves depend on the applied stress and the ageing temperature. It was noticed also that increasing temperature led to an increase in the steady state creep rate ( $\dot{\epsilon}_{st}^*$ ). Irregular variations in the levels of the creep curves especially around the region of transition were observed. By performing the creep tests for the quenched alloy samples (Pb-1.5wt% Sb) aged below 443K, both the  $\alpha$ -phase (Pb-rich phase) and the precipitated  $\beta$ -phase (Sb-rich phase)-light phase were observed. The  $\beta$ -phase dissolves in  $\alpha$ -phase with increasing the ageing temperature until the transition temperature 443 K, as was expected in accordance with the phase diagram [14]. This increase of solubility may be concluded from the observations of both transient and steady state creep rates at high temperature.

Figure (2) shows the relation between the transient strain creep  $\ln \epsilon_{tr}$  and  $\ln t$ , under the different applied stresses and temperatures ranging from 413K to 473K. Irregular arrangement of the straight lines at different temperatures is observed in this relation. Figure (3) shows the temperature dependence of the transient creep parameters ( $\beta$  and  $n$ ). A gradual increase in both transient creep parameters until 443K is noticed followed by a decrease above this temperature, then a final increase.

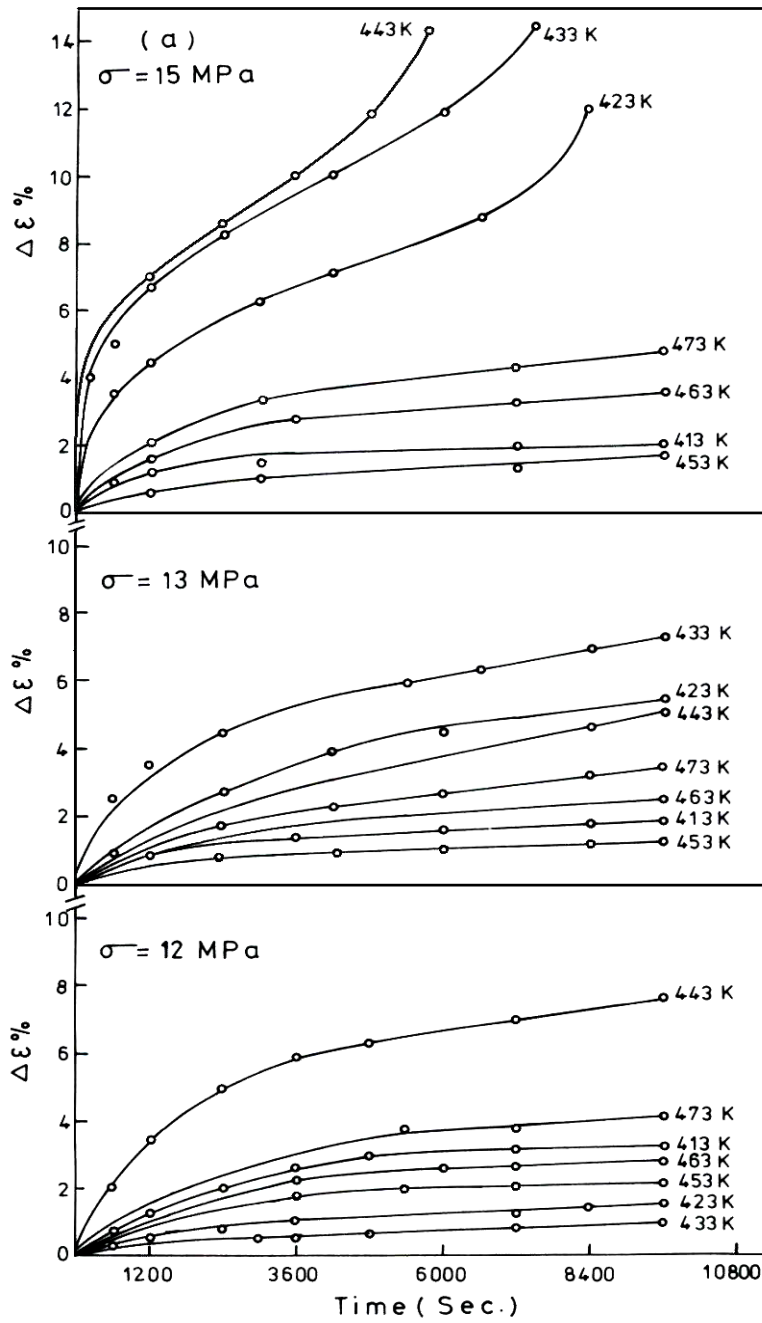


Fig. (1): The creep curves of (Pb-1.5 wt% Sb) quenched alloy under different constant applied stresses at different ageing temperatures.

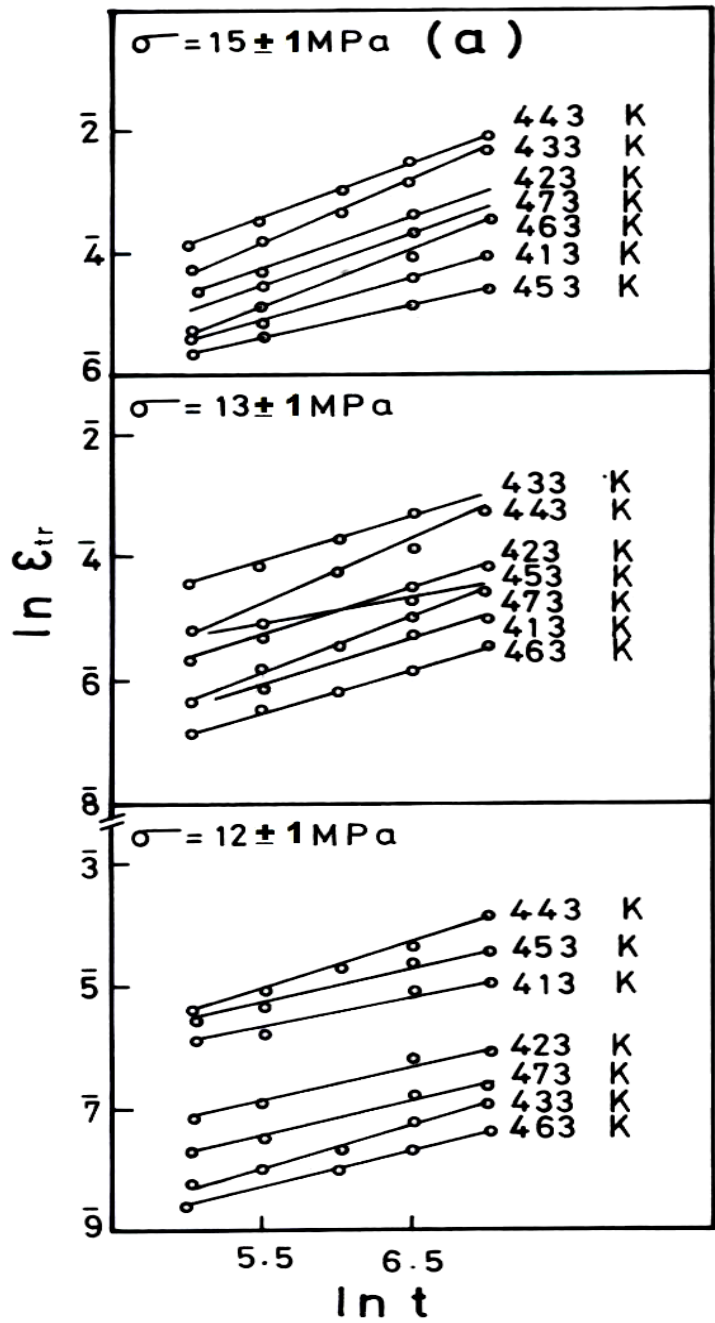


Fig. (2): Relation between  $\ln \epsilon_{tr}$  and  $\ln t$  for (Pb-1.5 wt% Sb) quenched alloy at different ageing temperatures and under different applied stresses

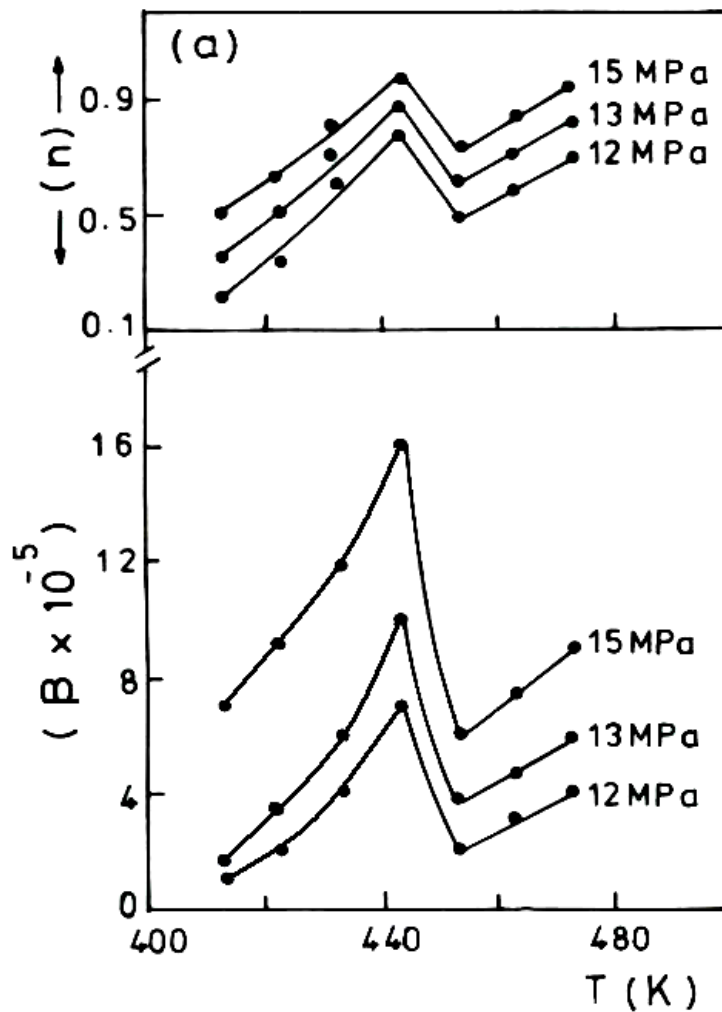


Fig. (3): The temperature dependence of the transient creep parameters  $\beta$  and  $n$  at different applied stresses for the quenched alloy (Pb-1.5 wt% Sb).

The above mentioned behaviour was attributed to redistribution of the precipitated Sb particles [15]. Increasing temperature up to the transition temperature causes a coarsening process of the  $\beta$ -phase. The diffusion of Sb atoms has a great effect on the motion of dislocations at the interphase boundaries [16] and new dislocation sources may be developed and cause rearrangement in the dislocation networks during phase transformation [17]. Above 443 K, the final increase in ( $\beta$  and  $n$ ) might be related to the dissolution of the Sb-rich phase and the relaxation of dislocations at the grain boundaries. This process may be associated with dislocation annihilation by thermal

agitation in this temperature range where a homogenized matrix is obtained [14]. The increased values of  $\beta$ ,  $n$  and  $\varepsilon_{st}^*$  (figs. 3 and 6) were explained by the viscous self-diffusion of Sb in this temperature range [16].

The activation energy of transient creep was calculated from the straight line relating  $\ln \beta$  and  $1000/T \text{ K}^{-1}$  as shown in Fig. (4). The present results yielded activation energies 52 kJ/mole and 92 kJ/mole in the temperature ranges above and below 443 K, respectively, characterizing a grain boundary sliding mechanisms [16].

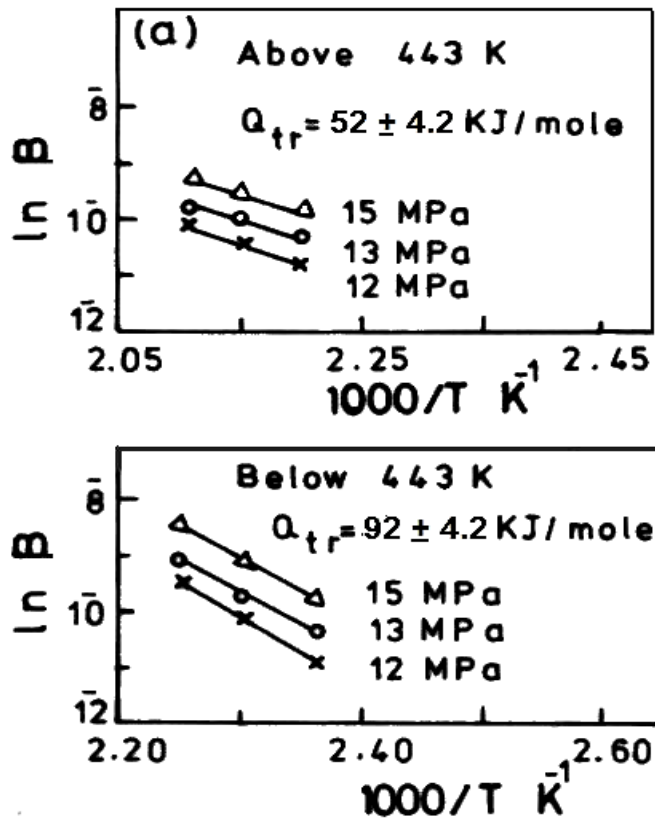
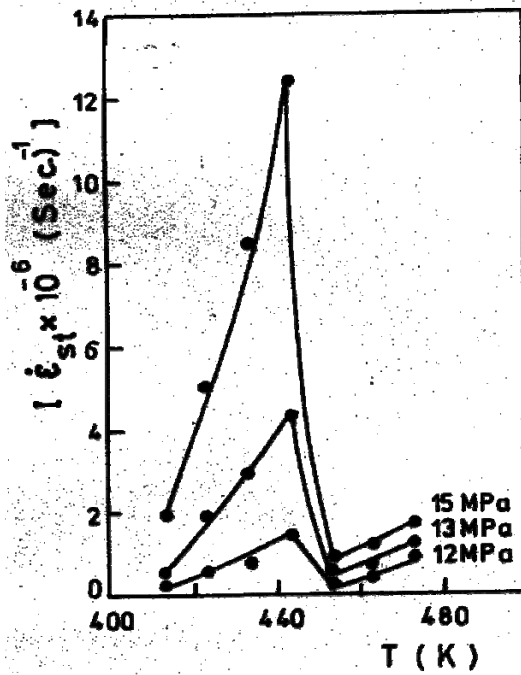


Fig. (4): The relation between  $\ln \beta$  and  $10^3/T \text{ K}^{-1}$  for the quenched alloy (Pb-1.5 wt% Sb) at different applied stresses.

Figure (5) shows the temperature dependence of  $(\varepsilon_{st}^*)$  where a gradual increase of  $(\varepsilon_{st}^*)$  until 443 K is observed. The steady state creep rate  $(\varepsilon_{st}^*)$  under the different applied stresses and different ageing temperatures was calculated from the slope of the linear parts of the creep curves given in Fig. (1).



**Fig. (5):** The relation between  $\dot{\epsilon}_{st}^*$  and different ageing temperatures at different applied stresses for the quenched alloy (Pb-1.5 wt% Sb).

The above mentioned behaviors may be attributed to the segregation of  $\beta$ -phase (Sb-rich phase) around the columnar structure for  $\alpha$ -phase (Pb-rich phase). The rapid increase for  $\dot{\epsilon}_{st}^*$  above 443K may be due to the dissolution of Sb-rich particles and then the alloys become homogenized.

A correlation between the transient and steady state creep state was obtained through the exponent  $\gamma$  from the relation:

$$\beta = \beta_o (\dot{\epsilon}_{st}^*)^\gamma \quad (1)$$

The relation between  $\ln \beta$  and  $\ln \dot{\epsilon}_{st}^*$  was plotted in Fig. (6). Connecting  $\beta$  and  $\dot{\epsilon}_{st}^*$  seems to be valid with the exponent ( $\gamma$ ),  $\gamma = 0.55$ . The dependence of the strain rate of steady state creep ( $\dot{\epsilon}_{st}^*$ ) on ( $\beta$ ) seems to be induced by the phase transformation which enhances the transient and the steady state stages [18].

Figure (7) shows the stress dependence of the ( $\varepsilon_{st}^*$ ) from which the strain rate sensitivity parameter ( $m = \partial \ln \delta / \partial \ln \varepsilon_{st}$ ) was calculated from the slope of the straight line.

Figure (8) gives the temperature dependence of ( $m$ ). It was found that ( $m$ ) increases with increasing temperature, having values ranging from (0.11 to 0.33). These may be attributed to both cross-slipping and climb dislocation mechanisms [19].

The activation energies of the apparent steady state creep ( $Q_{st}$ ), were calculated from the relation between  $\ln \varepsilon_{st}^*$  and  $1000/T$  shown in Fig. (9). They were found to depend on the temperature range and the applied stress. They have values of 101 kJ/mole above 443 K and 92 kJ/mole below 443 K. These values may refer to viscous creep [15]. This shows that in the low and high temperature range, relative to transition temperature (443 K), the steady state creep is governed by a thermally activated and stress assisted processes.

Figure (10) shows the X-ray diffractometry study for initial quenched and crept samples of (Pb -1.5wt% Sb) alloy in the range of diffraction angle  $2\theta$  ( $30^\circ - 92^\circ$ ). These patterns illustrate the existence of the Pb-matrix. The variation in the two peaks intensity of Pb (111) and Pb (200) might be attributed to the grain - orientation effects [20].

Figure (11) shows the relation between the integral intensity (**I**) and the half line width at maximum intensity ( $\Delta 2\theta$ ) for crept alloy samples at different temperatures. It is found that (**I**) and ( $\Delta 2\theta$ ) increase with increasing the ageing temperature until 443 K, after which they decrease until 453 K, then increase again. The first increase until 443 K is attributed to the increase of the dissolution rate of the solute atoms (Sb) in  $\alpha$ -phase (Pb-rich phase) by a thermally activated and stress assisted force. The first decrease in their values to minima indicates that the residual internal lattice strain decreased appreciably in the  $\alpha$ -phase owing to the relaxation process of the cross-slipping dislocation [21].

Figure (12) shows the isothermal resistivity change ( $\rho_t/\rho_o$ ) with temperature 393 - 473 K, where ( $\rho_o$ ) is the initial value of the specific electrical resistivity immediately after quenching in liquid nitrogen. The change of resistivity was calculated at different ageing times to follow the various precipitation and dissolution process during the ageing of the test samples at

different ageing temperatures. In the temperature range 393 - 413 K,  $(\rho_t/\rho_o)$  increases with increasing the ageing time depending on the ageing temperature. A slight decrease of  $(\rho_t/\rho_o)$  against time (t) was observed followed by constant values independent of time. In the temperature range (443 - 473) K, the isothermal resistivity ratio  $(\rho_t/\rho_o)$  decreases with increasing ageing time depending on the ageing temperature. Then a slight increase of  $(\rho_t/\rho_o)$  followed by constant values independent of time is observed. The maximum value of  $(\rho_t/\rho_o)$  was found to depend on the ageing temperature and ageing time. At temperature 433 K, which is below 443 K,  $(\rho_t/\rho_o)$  is slightly increasing with increasing the ageing temperature.

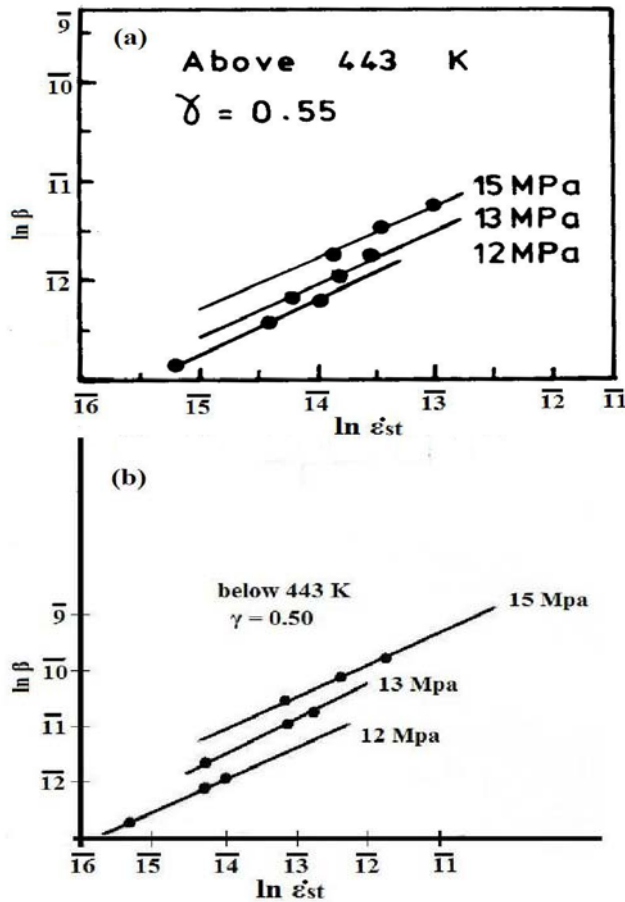


Fig. (6): The relation between  $\ln \beta$  and  $\ln \epsilon_{st}$  for the quenched alloy (Pb-1.5wt% Sb).

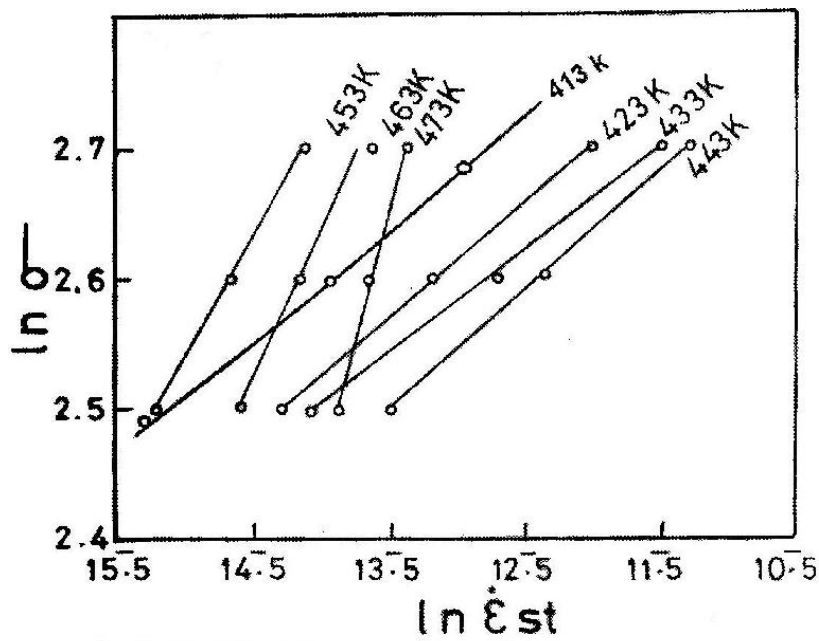


Fig. (7): The relation between  $\ln \sigma$  and  $\ln \dot{\epsilon}_{st}$  at different ageing temperatures for the quenched alloy (Pb-1.5 wt% Sb).

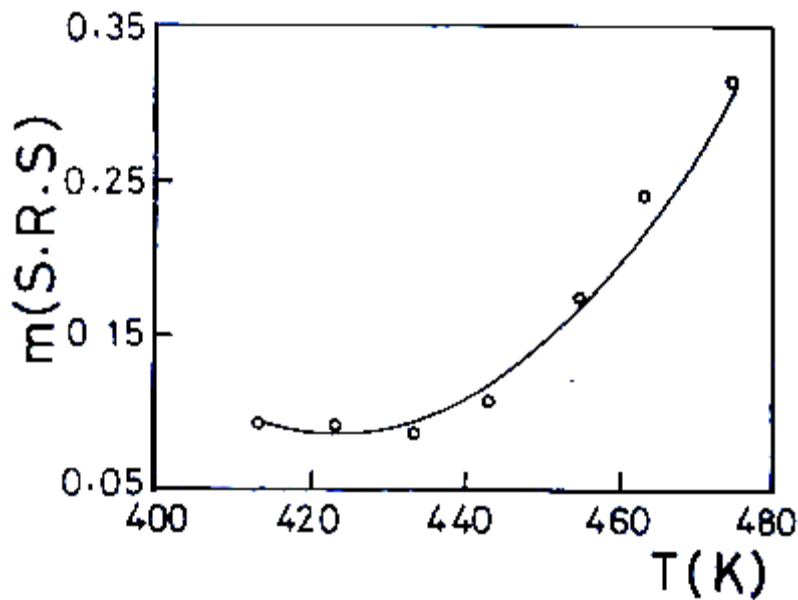


Fig. (8): The relation between the strain rate sensitivity parameter ( $m$ ) and the different ageing temperatures for (Pb-1.5 wt% Sb) quenched alloy ( $T_q = -20^\circ C$ ).

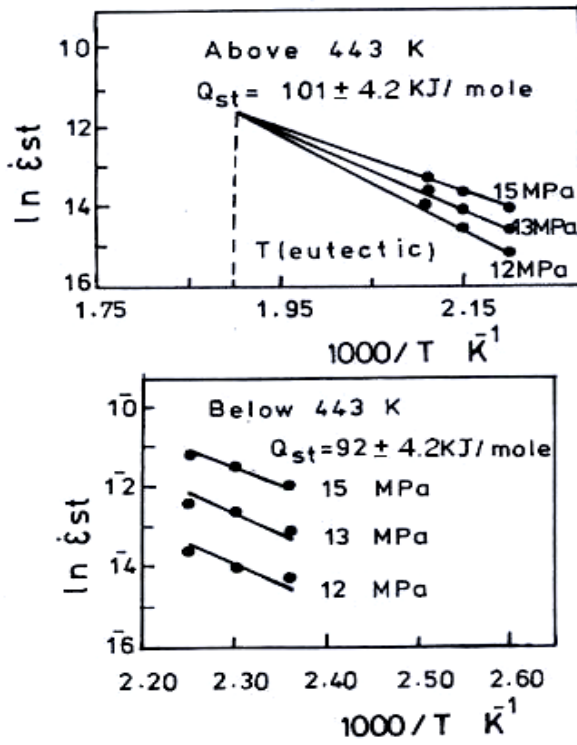


Fig. (9): The relation between  $\ln \epsilon_{st}$  and  $10^3/T \text{ K}^{-1}$  at different applied stresses for (Pb-1.5 wt% Sb) quenched alloy.

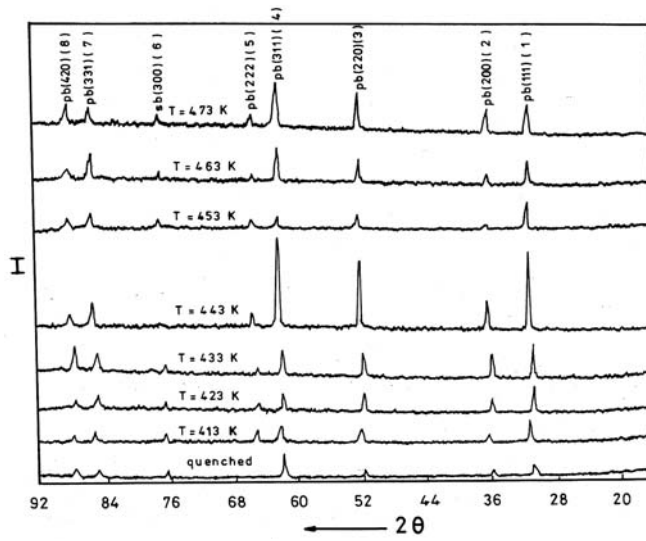


Fig. (10): X- ray diffraction pattern for (Pb-1.5 wt% Sb) quenched alloy after creep under applied stress 15 Mpa at different ageing temperatures.

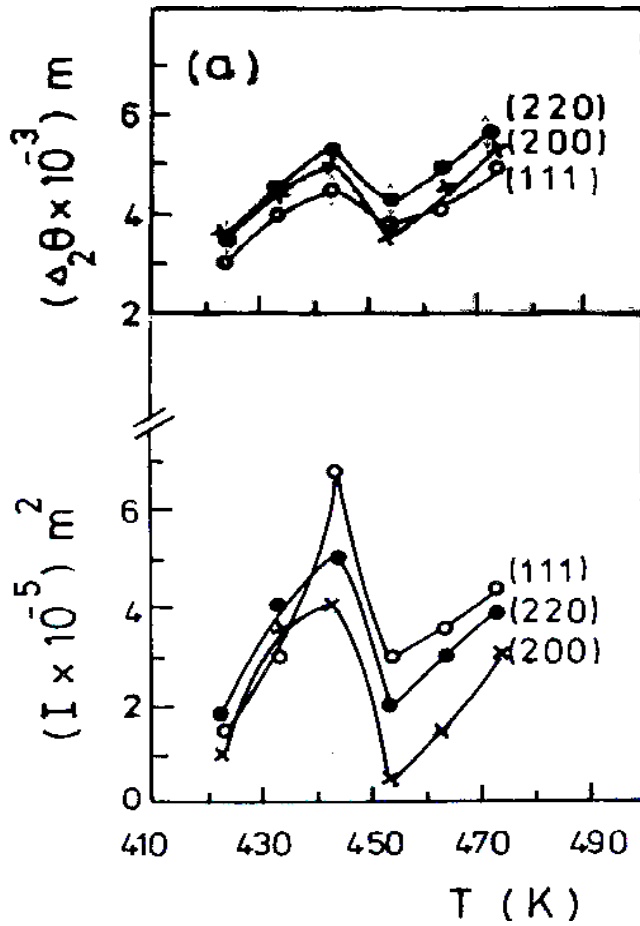


Fig. (11): The effect of different ageing temperatures on the integral X-ray intensity (I) and the half line width ( $\Delta\theta$ ) for (Pb-1.5 wt% Sb) quenched alloy.

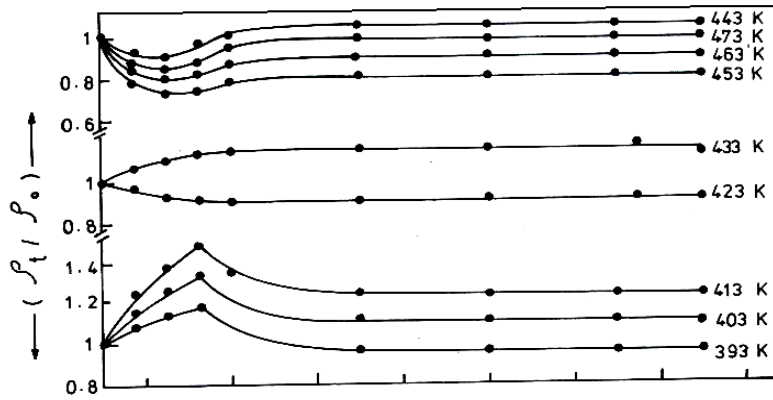


Fig. (12): Time dependence of isothermal resistivity ratio ( $\rho_t / \rho_o$ ) for (Pb-1.5 wt% Sb) quenched alloy.

These behaviors might be due to the formation of the fine precipitated particles (Sb-rich phase) where they act as scattering centers for the conduction electrons. The decrease of the ratio  $(\rho_i/\rho_o)$  at temperature 423K with increasing the ageing time might be attributed to the slight annihilation of quenched-in vacancies, i.e. decreasing the number of scattering centers for the conduction electrons [22]. Also, the slight increase in  $(\rho_i/\rho_o)$  with increasing ageing time could be attributed to the enhancement of the quenched-in vacancies which act as the scattering centers.

The activation energy of the formation and dissolution processes of (Sb-phase) in each ageing stage below and above 443 K, was calculated from the linear change of the relation between  $\ln(\rho_i/\rho_o)$  versus  $10^3/T(K^{-1})$  for different ageing times as in Fig. (13). The values of the activation energy were found to be (0.11 and 0.12) eV, above and below 443 K, respectively. These values correspond to the binding energy between the quenched vacancy and (Sb) solute atom [23].

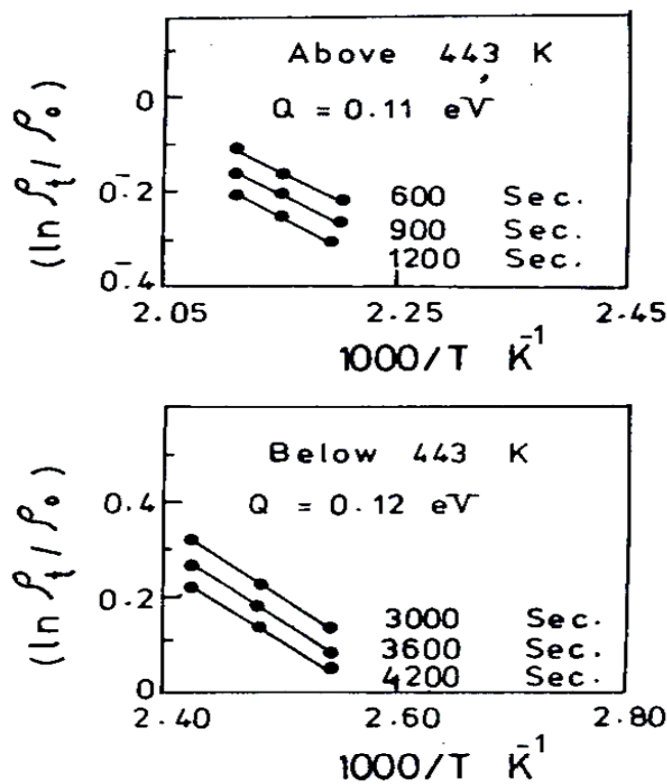
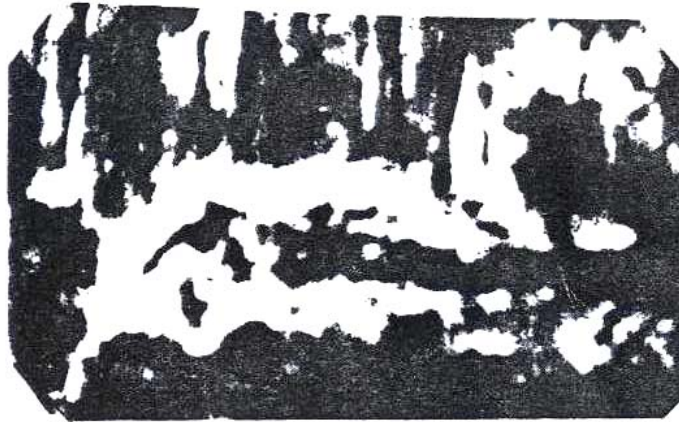


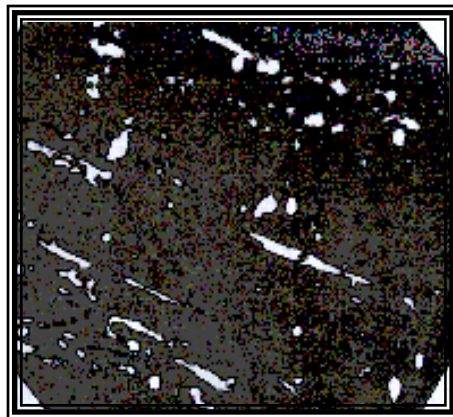
Fig. (13): The relation between  $\ln(\rho_i/\rho_o)$  and  $10^3/T \text{ K}^{-1}$  at different ageing times for (Pb-1.5 wt% Sb) quenched alloy.

Figure (14), shows the microstructure investigation for the studied alloy aged at 443 K. It is clear that the segregation of  $\beta$ -phase (Sb-rich phase) (light) takes place around the columnar grains of the dark phase (Pb-rich phase), thus the number of pinning dislocation points within the grain will decrease and hence the creep rate will increase until 443 K.



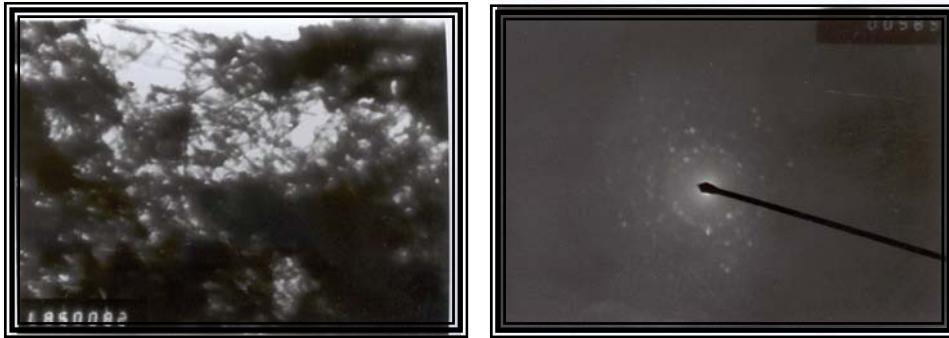
**Fig. (14):** Scanning electron micrograph for quenching sample of (Pb-1.5 wt% Sb) alloy homogenized at 443 K for 72h. Showing a final segregation of (Sb) solute, light phase, around the columnar dark phase (Pb). (Mag. X = 15000).

Figure (15) shows the microstructure for the studied alloy at the highest temperature 473K, where redistribution of  $\beta$ -phase (Sb-rich phase) in the matrix is observed. Thus, the creep rate will increase due to the decrease in pinning points of dislocations within the grain.



**Fig. (15):** Scanning electron micrograph for quenching sample of (Pb-1.5 wt% Sb) alloy annealed at 473 K for 2 h. Showing the  $\beta$ -phase, Sb-rich phase, will be redistribution in the matrix. (Mag. X = 10000).

Figure (16) shows the electron micrograph and electron diffraction patterns of the studied alloy at 433K showing that the  $\beta$ -phase (Sb-rich slute) is segregated around the  $\alpha$ -phase (Pb-rich phase), having a columnar shape, hence the creep rate is increased.



**Fig. (16):** Electron micrograph (Mag. X = 25000) and corresponding diffraction pattern for quenching sample of alloy (Pb-1.5 wt% Sb) annealed at 433 K for 2 h. Showing: Dark phase ( $\alpha$ -phase) Pb-rich phase and Light phase ( $\beta$ -phase) Sb-rich solute.

#### 4. Conclusion:

The obtained results of tensile deformation transient creep, steady state creep of the quenched alloy (Pb - 1.5wt % Sb) showed a transition point at 443K. The strain rate sensitivity parameter ( $m$ ) was found to be in the range 0.11-0.33 pointing to both cross slipping and climb dislocation mechanisms. The activation energies of the transient creep were found to be 52 and 92kJ/mole above and below the transition temperature characterizing grain boundary sliding mechanism. The activation energies of the steady state creep for the studied alloy were found to be 101, and 92 kJ /mole above and below 443K respectively, characterizing the viscous creep mechanism. X-ray investigation of the crept samples shows that the internal residual strains exhibit a peak value at 443K. The activation energies of the formation and dissolution of precipitates in the studied alloy as calculated from resistivity changes were found to be of the order of magnitude of the binding energy between quenched vacancy and Sb- solute atom. The extremely high cooling rate and increased solid solubility associated, produce, microstructure with a heterogeneous distribution of unconventional and non - equilibrium phase .This enhanced the creep rate.

**References:**

1. J. J. Londer, *J. Electrochemist. Soc.*, **99**, 339, (1952).
2. J. L. Dowson, M. I. Gilliland and J. Wilkinson, 1, "7<sup>th</sup> International Power Sources", Symposium, Barrington, England, (1970).
3. W.Hofmann, "Lead and Lead Alloys". Springer - Verlag, New-York and Berlin, p. 341 (1970).
4. J. Perkins and G.R. Edwards, *J. Mat. Sci.*, **10**, 136, (1975).
5. A. Cameron, "The Principles of Lubrication", Longman, London, p. 263, (1966).
6. R. Alarshi, A.M. Shaban and M. Kamal, *Materials letters*, **31**, 61, (1997).
7. R.E. Smallman, "Modern Physical Metallurgy", London, p. 293 (1962).
8. M.M.Mostafa, *Physica B*, **56**, 349, (2004).
9. G.S. Al Ganainy, M.T.Mostafa and F. Abd El-Salam, *Physica B* **438**, 244 (2004).
10. E.M. Sakr, M.R. Nagy and A.S. Mahmoud, *Egypt. J. Solids*, **29**, 1 (2006).
11. M.S. Sakr, *phys. stat. sol. (a)*, R **37**, 126 (1991).
12. B.D.Culity, "Element of X-ray diffraction", Addison - Wesley Public – Co. (1956).
13. M. Amin, G.M. Nasr, S.A. Khairy and E.A. Ateia, *Die angewants makromolekulare, chemi*, **19**, 2274, 141 (1986).
14. M. Hansen, Constitution of binary alloys, MC.Grow-Hill Publ. Co., New York (1958).
15. G.S. AL- Ganainy, M.T. Mostafa and M.R.Nagy, *phys. stat. sol. (a)*, 165, 185, (1998).
16. P. Lukac, A.G. Malygin and V.A Vlodymirova, *Czech. J. Phys. B*, **35**, 318 (1985).
17. M.S. Sakr, A.E.E Abd - El - Raheim and A.A. El-Dally, *phys. stat. sol. (a)* **89**, K 157, (1985).
18. M.S. Sakr, A.A.EL -Shazly, M.M. Mostafa and H.A. El-Said, *Czech .J.Phys.*, B38, (1988).
19. A. Ball and M.M Hutchison, *Metal. Sci. J.*, **3**, 1, (1969).
20. N.B Dahotre, M.H. Mc Cay, T.D. Mc Cay and M.M kim , *J. of Mat .Sci.*,27,6426 , (1992) .
21. M.S. Sakr, A.E.E .Abd-El-Reheim and A. A.El-Dally, *phys. stat. sol. (a)*, **94**, 561, (1986).
22. M. M. Mostafa, A. A. El - Shazly, M.S. Sakr and H. A. EL-Sayed, *Egypt. J. Solids*, **2**, 15 (1992).
23. J. Szablewski and B. Kuznich, *Mat. Sci. and Tech.*, **7**, 407, (1991).